

# Effects of slice thickness and head rotation when measuring glioma sizes on MRI: in support of volume segmentation versus two largest diameters methods

Pierre Schmitt · Emmanuel Mandonnet ·  
Adrien Perdreau · Elsa D. Angelini

Received: 2 August 2012 / Accepted: 29 December 2012 / Published online: 9 February 2013  
© Springer Science+Business Media New York 2013

**Abstract** This paper presents a study of the effects of scanning parameters variability when assessing glioma sizes on MRI. A database of lesions of various shapes and sizes, segmented on 3D-SPGR MRI images, was acquired on 65 patients with low-grade glioma. Simulations of large slice thickness and patient's head rotation were performed, allowing us to study their influence on two size indices: the bi-dimensional diameter product index (computed with the two largest diameters method) and the equivalent diameter index (computed with the volume segmentation method). Results show that thick slices and axial plane rotation can induce average (maximal) uncertainties on the bi-dimensional diameter product index between 32 and 6 % (150 %) for small and large tumors (size range 0.5–286 ml). The uncertainty on the equivalent diameter index, for the same categories of tumors, drops below 8 and 0.1 % (23 %). This study shows that the volume segmentation method is subject to less variability inherent to scanning conditions compared to the two largest diameters method. It also emphasizes the need for strict clinical guidelines on the replication of scanning conditions when performing MRI follow-ups on patients harboring small tumors. These

implications await confirmation on a series of real patients being re-scanned with FLAIR MRI.

**Keywords** MRI · Brain tumor · Low-grade glioma · Longitudinal growth quantification

## Introduction

Assessing the evolution of tumor size by morphological longitudinal MRI follow-up plays a prominent role in neuro-oncology. This holds especially true for diffuse low-grade glioma, as radiological evolution is often the only measure available to capture the disease progression before treatment [1–3], after surgery [4], after chemotherapy [5, 6] or after radiotherapy [7].

Testifying to the importance of the analysis of radiological changes on MRI when evaluating treatment efficacy, the response assessment in neuro-oncology (RANO) group recently updated the original definition of the MacDonalds criteria of radiological response for the specific case of low-grade glioma [8]. These revised criteria now rely on the measure of the two largest tumor diameters (i.e. linear measurements). Other authors recommend a full 3D-segmentation of the tumor on all available axial slices (i.e. perimeter method), leading to an estimation of the tumor volume, from which an equivalent spherical diameter can be computed [9]. Two arguments support the latter approach:

- It has been clearly shown that perimeter-based methods are less subject to intra- and inter-rater variability on a large series of high-grade glioma [10],
- Equivalent diameter evolution of diffuse low grade gliomas (DLGG) appears to be linear, thus facilitating

---

P. Schmitt · A. Perdreau · E. D. Angelini (✉)  
Institut Mines-Telecom, Telecom ParisTech, CNRS LTCI,  
46 Rue Barrault, 75013 Paris, France  
e-mail: elsa.angelini@telecom-paristech.fr

P. Schmitt  
e-mail: pierre.schmitt@telecom-paristech.fr

A. Perdreau  
e-mail: adrien.ap.perdreau@gmail.com

E. Mandonnet  
Neurosurgery Department, Hôpital Lariboisière, Paris, France  
e-mail: mandonnet@mac.com

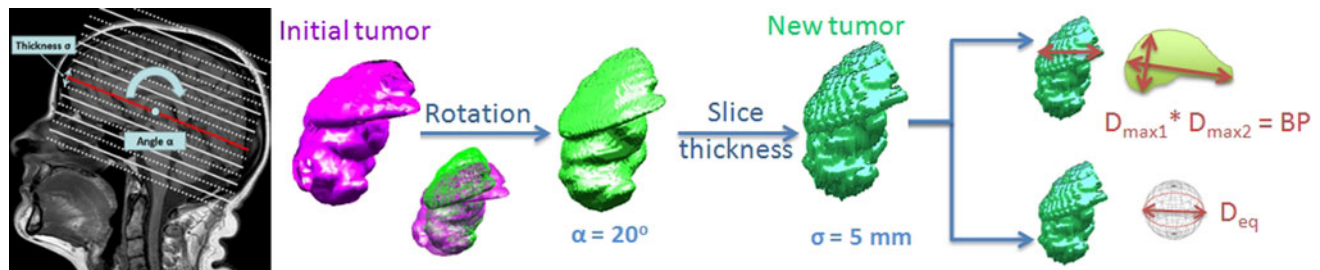


**Fig. 1** Illustration of MRI scanning conditions and pipeline of the reslicing of binary segmented volumes, illustrated on a tumor from our database. Two parameters are controlled: (1) the orientation of the

the estimation of annual growth rates from a pair of successive images [11].

However, the influence of the variability in MRI scanning setup and imaging parameters on these distinct indices of glioma size remains unknown. In this work, we studied two sources of variations in the scanning conditions: rotation of the reference axial plane (i.e. patient's head rotation) and modification of the slice thickness, as illustrated in Fig. 1.

By generating images simulating different image acquisition conditions, we sought to quantify their influence on the measures of the two main size indices used to monitor radiological DLGG evolution.

## Material

**Patients:** a database of 65 patients with low-grade (WHO grade II) glioma was used. This database was extensively described in [12]. Patients were all treated with surgery. Tumoral resection was either total or partial (i.e. with residual volume above 10 ml) if the tumor infiltrated functional areas. MRI images were acquired either immediately after surgery (25 cases), or between 3 to 6 months after surgery (40 cases).

**MRI data:** MRI data was acquired on a 1.5 T scanner with a 3D-SPGR sequence, and a voxel spatial resolution of  $1 \times 1 \times 1 \text{ mm}^3$ . Low-grade glioma are non-enhancing tumors, that display on SPGR images darker intensities than the surrounding white matter. Resection cavities have intensities corresponding to the dark CSF.

**Manual segmentation:** manual segmentation was performed by an expert neurosurgeon on 3D-SPGR MRI data. Both the lesion and the residual tumor were segmented, as detailed in [12]. By definition, the lesion is considered to be the combination of the residual tumor and the resection cavity. Only 56 patients had some residues visible on the MRI data.

**Lesion and residue volumes:** lesions and residues covered a wide range of shapes and volumes, with the following volume values (av. stands for average):

axial plane via a rotation (by an angle of  $\alpha$ ) around an axis perpendicular to the sagittal plane direction, and (2) the axial slice thickness ( $\sigma$  in mm)

- Lesions: av. = 96.7 ml, min = 3.7 ml, max = 286.4 ml.
- Residues: av. = 11.3 ml, min = 0.5 ml, max = 62.0 ml.

This large variety of shapes and sizes provided a diverse set of cases to study the effect of scanning parameters on the measurement of tumor sizes. Indeed, longitudinal monitoring of tumor expansion is required for both initial lesions (potentially large and with roughly bulky shapes) and residues (potentially small and elongated along the resection margins). We therefore studied size measurements on both segmented lesions and residues as a group of 121 segmented tumors encoded on binary masks with values 0 and 1.

## Method

### Simulation of scanning conditions via reslicing

We generated several series of new segmented tumors from the reference binary masks containing the manual contours traced by a neurosurgeon on 3D-SPGR MRI scans acquired at high spatial resolution (voxel size of  $1 \times 1 \times 1 \text{ mm}^3$ ). Simulation of new scanning conditions involved three computational steps illustrated in Fig. 1, which define the following reslicing pipeline:

- (1) Rotation of the tumor, performed on the binary volume.
- (2) Selection of the position of the first slice along the direction orthogonal to the axial plane which we will call the axial direction.
- (3) Aggregation of adjacent slices to generate thicker ones.

Rotation of the binary masks was applied around the direction orthogonal to the sagittal plane, with an angle of  $\alpha$  degrees. It was performed using tri-linear interpolation and thresholding of the interpolated pixel intensity values at 0.5.

For MRI acquisitions with large slice thickness, even if the axial plane orientation is preserved, slice positions can be shifted, depending on the selection of the position of the

first axial slice. We therefore simulated large slice thickness volumes with  $n$  different shifts (in mm) of the axial slice position for a slice thickness of  $n$  mm.

Aggregation of adjacent slices was performed via slice averaging, as in [13], with uniform odd-length kernels of size 3, 5 and 7 mm in the axial direction. The size of the averaging kernel corresponded to the new slice thickness ( $\sigma$  mm). Odd sizes were used to have symmetric kernels and therefore evenly aggregate the image information contained below and above the new axial slice. Thresholding was applied on the averaged slices to generate new binary segmented volumes. Thresholding was based on a majority voting fusion (MVF) rule, setting a voxel to 1 if its value was 1 in at least half of the combined slices. The MVF rule corresponds to a threshold value of the averaged slices set to 0.5.

Computation of tumor size indices

For each series of simulated binary volumes containing segmented tumors, we computed the tumor volume  $V_T$  (in ml) by counting the number of voxels of value 1. Two different tumor indices (and associated computation methods) were used to characterize the tumor size:

- The bi-dimensional diameter product (also known as the MacDonald index):
  - *value*: product of the two orthogonal maximum diameters, measured on the axial slice with the largest bi-dimensional product (in  $\text{mm}^2$ ).

- *notation*:  $BP$  (for bi-dimensional product).
- The equivalent diameter:
  - *value*: diameter of the sphere having a volume equal to  $V_T$  (in mm).
  - *notation*:  $D_{eq}$  (for diameter equivalent).

Comparison of tumor size indices

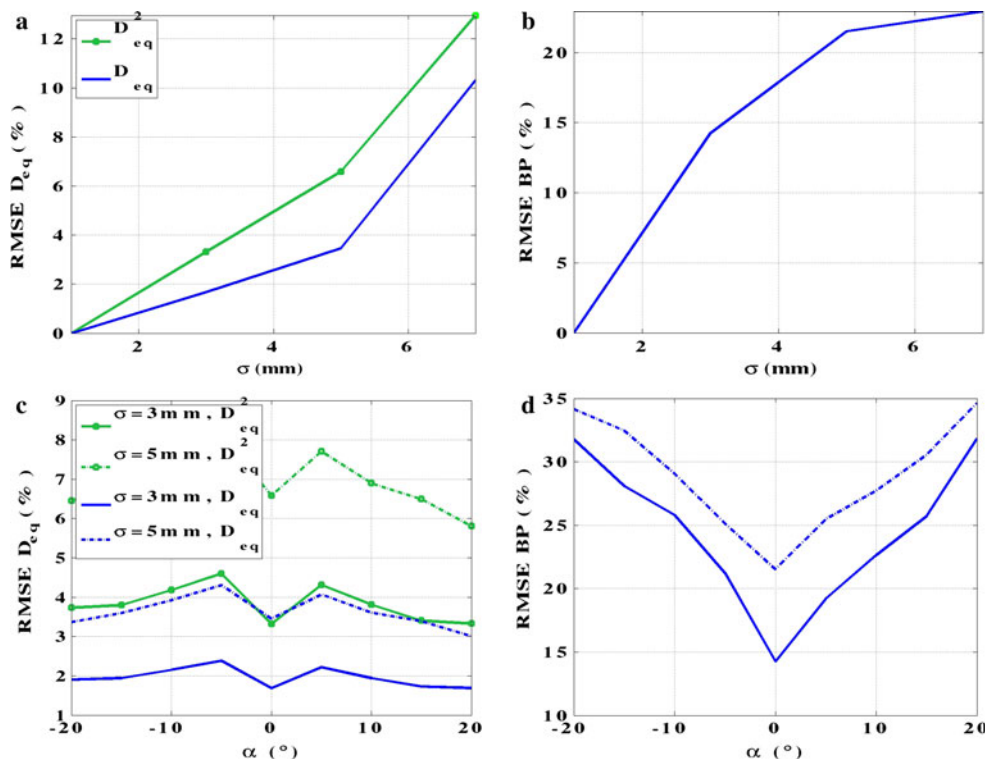
The root mean squared errors (RMSE) of  $D_{eq}$  and  $BP$  were computed by comparing the values measured on the original (reference) volumes and the resliced volumes.

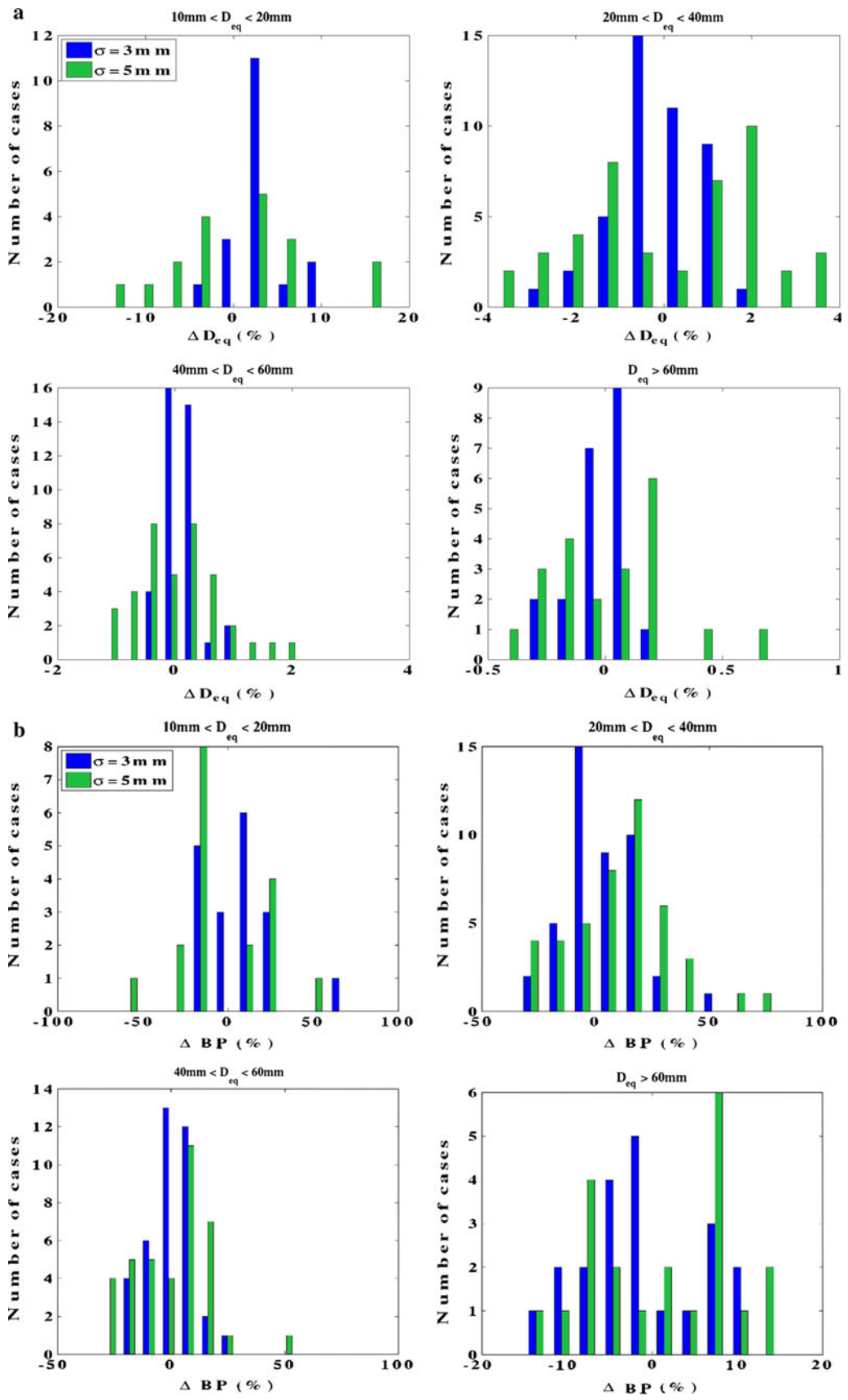
The values of the signed differences, denoted  $\Delta D_{eq}$  and  $\Delta BP$ , subtracting the estimate on the original volume from the estimate on the resliced volume were determined for all cases. A negative  $\Delta D_{eq}$  value therefore corresponds to an underestimation of the tumor size, after reslicing.

To better understand the meaning of these errors, their values are expressed in percentage with respect to the original value of the studied index.

We clustered the database of the 121 tumors (either residues or lesions) into four categories, based on their  $D_{eq}$  value, as follows:  $C_1 = \{10\text{mm} \leq D_{eq} < 20\text{mm}\}$ ,  $C_2 = \{20\text{mm} \leq D_{eq} < 40\text{mm}\}$ ,  $C_3 = \{40\text{mm} \leq D_{eq} < 60\text{mm}\}$ ,  $C_4 = \{D_{eq} \geq 60\text{mm}\}$ . The repartition of cases in each group was the following:  $C_1$  (18),  $C_2$  (44),  $C_3$  (38) and  $C_4$  (21). These categories will be used to report the variability of tumor size index measurements and assess the potential

**Fig. 2** Average RMSE of  $D_{eq}$ ,  $D_{eq}^2$  and  $BP$  index measures. **a**, **b** RMSE versus slice thickness  $\sigma$ . **c–d** RMSE versus rotation by an angle of  $\alpha^\circ$  of the axial plane, combined with different slice thickness values  $\sigma$





◀ **Fig. 3** Histograms of errors for slice thickness  $\sigma = 3$  mm (blue) and  $\sigma = 5$  mm (green) for the four categories of tumor volume size. **a** Errors on  $\Delta D_{eq}$ . **b** Errors on  $\Delta BP$ . Signed errors all verify the t-test for being centered except for *BP* in class *C1* (at  $p \leq 0.05$ )

influence of the initial tumor size on their sensitivity to scanning conditions.

### Results

#### Effect of slice thickness increase

Changing the slice thickness was combined with testing different shifts of the axial slices. We compared size indices for slice thickness value  $\sigma = 1$ mm versus  $\sigma = 3, 5$  or  $7$ mm and report maximal error over all possible shift values, for a given slice thickness.

We plotted in Fig. 2a, the RMSE values versus  $\sigma$  to visualize the average effect of the slice thickness on the tumor size index measures. At  $\sigma = 7$ mm, a maximal RMSE of 10 % for  $D_{eq}$  and 22 % for *BP* was obtained. We also plotted the RMSE of  $D_{eq}^2$  to enable direct comparison of the indices with homogeneous units of  $\text{mm}^2$ . The maximal RMSE of  $D_{eq}^2$  over  $\sigma$ , reaching 13 % was still below the maximal RMSE of the *BP* index. Histograms of  $\Delta D_{eq}$  and  $\Delta BP$  values over the four tumor size categories are reported in Fig. 3a,b for two slice thickness values ( $\sigma = 3$  or  $5$ mm). These histograms confirm larger average and maximum errors for larger slice thickness. They also show a higher sensitivity of *BP* compared to  $D_{eq}$ , especially for small tumor sizes ( $C_{1-3}$  classes) where the maximal uncertainty in the size index varies between 50 and 100 %. Average and maximal  $|\Delta D_{eq}|$  and  $|\Delta BP|$  values, in percent and millimeters, for each tumor size category, are reported in Tables 1 and 2. From these results, we can summarize the following observations:

- Larger slice thickness introduces less uncertainty in the  $D_{eq}$  index compared to the *BP* index.
- For the  $D_{eq}$  measure, small tumors are more affected than large ones. This is especially important when considering the maximal potential error: 0.3 to 4.0 % for tumors in categories  $C_2, C_3, C_4$  versus 10.6 to 17.5 % for tumors in category  $C_1$ . For the *BP* measure, all tumor categories are affected by a large maximal error from 150.3 to 79.7 %.
- Comparing errors for a given scanning condition, the mean values of errors for  $D_{eq}^2$  are statistically similar or smaller ( $p \leq 0.05$ ) than for *BP* for all tumor size categories.
- A test on the variance of the signed errors shows that the variances for  $\Delta BP$  are statistically different ( $p \leq 0.005$ ) and greater than the variances for  $\Delta D_{eq}^2$  for centered

differences (i.e. mean of errors being subtracted), for all classes except  $C_1$ , for which they are statistically equal ( $p \leq 0.005$ ).

- The means of errors for  $D_{eq}$  can explain ( $p \leq 0.005$ ) the means of errors for *BP* (with different variances). Means of errors are not 0 and should therefore be checked with table values provided by such study.
- Regarding the comparison of scanning conditions for a given index measure, the means of errors clearly remain larger for *BP* than for  $D_{eq}^2$ , and both increase with larger  $\sigma$ .

#### Effect of axial plane orientation

We illustrate in Fig. 2c,d the average RMSE values for  $D_{eq}$  and *BP* size indices comparing measures before and after rotations of the axial plane by an angle  $\alpha$  in the range  $[-20^\circ + 20^\circ]$  with a  $5^\circ$  increment. RMSE plots are provided for different slice thickness values and for the shift of the position of the first axial slice generating maximal error. We observed symmetric effects of positive and negative rotations on the RMSE values. The level of the RMSE for  $D_{eq}$  remains small as the rotation angle increases (between 1.5 and 2.5 % when  $\sigma = 3$ mm and between 3 and 4 % when  $\sigma = 5$ mm). *BP* however is more affected by the rotation and reaches a maximal RMSE of 35 % as rotation angle increases. In all cases, the maximal RMSE for *BP* remains higher than the maximal RMSE for  $D_{eq}^2$  (5 and 8 % for  $\sigma = 3$  and  $5$ mm).

Histograms similar to those in Fig. 3 were obtained (but are not shown in this article) when studying the signed errors  $\Delta D_{eq}$  and  $\Delta BP$  for a rotation of the axial plane by an angle  $\alpha$  in the range  $[-20^\circ + 20^\circ]$ , combined with a slice thickness increase of  $\sigma=3$  or  $5$ mm. Average and maximal  $|\Delta D_{eq}|$  and  $|\Delta BP|$  values, in percent and millimeters, for each tumor size category, are reported in Tables 1 and 2. From these results, we can summarize the following observations:

- Adding axial plane rotation to large slice thickness leads to a systematic increase (by 5–11 %) of errors for the *BP* index, while the errors for the  $D_{eq}$  index remain stable (increase by 0.1–0.9 %).
- Small tumors are the most affected by axial plane rotation, for both size index measures.
- Larger slice thickness leads to larger effects of the axial plane rotation on the uncertainty of the tumor size index measures.
- Increasing the amplitude of the axial plane rotation can increase, decrease or preserve the size index measures  $D_{eq}$  and *BP*, depending on the shape of the tumor.

**Table 1** Average and upper bound uncertainties (in percent) of size index measures with respect to (w.r.t.) different scanning conditions:  $\sigma = 3$  or 5 mm and  $\alpha$  in the range  $[-20^\circ, 20^\circ]$ 

$ \Delta D_{eq} $ (%)	Average				Max			
	$C_1$	$C_2$	$C_3$	$C_4$	$C_1$	$C_2$	$C_3$	$C_4$
w.r.t. $\sigma = 3$ mm	3.2	0.8	0.2	0.1	10.6	2.5	1.0	0.3
w.r.t. $\sigma = 3$ mm and $\alpha$	4.1	1.0	0.3	0.1	13.5	3.5	1.0	0.3
w.r.t. $\sigma = 5$ mm	6.9	1.7	0.6	0.2	17.5	4.0	2.1	0.7
w.r.t. $\sigma = 5$ mm and $\alpha$	7.5	1.9	0.7	0.3	22.8	5.7	2.3	0.8
$ \Delta BP $ (%)								
w.r.t. $\sigma = 3$ mm	16.0	12.7	7.8	6.1	71.9	52.8	23.9	14.1
w.r.t. $\sigma = 3$ mm and $\alpha$	25.8	24.0	16.1	11.6	94.5	150.3	77.4	37.8
w.r.t. $\sigma = 5$ mm	24.3	20.6	14.0	7.3	63.8	79.7	55.0	15.2
w.r.t. $\sigma = 5$ mm and $\alpha$	1.6	29.5	20.6	13.2	68.6	121.6	77.4	41.5

**Table 2** Average and upper bound uncertainties (in mm and  $\text{mm}^2$ ) of size index measures with respect to (w.r.t.) different scanning conditions:  $\sigma = 3$  or 5 mm and  $\alpha$  in the range  $[-20^\circ, 20^\circ]$ 

$ \Delta D_{eq} $ (mm)	Average				Max			
	$C_1$	$C_2$	$C_3$	$C_4$	$C_1$	$C_2$	$C_3$	$C_4$
w.r.t. $\sigma = 3$ mm	0.51	0.23	0.12	0.07	1.97	0.70	0.48	0.23
w.r.t. $\sigma = 3$ mm and $\alpha$	0.65	0.28	0.15	0.09	1.97	1.02	0.48	0.23
w.r.t. $\sigma = 5$ mm	1.07	0.48	0.29	0.15	3.07	1.0	1.01	0.47
w.r.t. $\sigma = 5$ mm and $\alpha$	1.16	0.54	0.35	0.23	3.35	1.24	1.11	0.53
$ \Delta BP (\text{mm}^2)$								
w.r.t. $\sigma = 3$ mm	64	130	211	375	255	458	807	1407
w.r.t. $\sigma = 3$ mm and $\alpha$	110	250	449	663	642	1342	3449	2580
w.r.t. $\sigma = 5$ mm	100	224	403	430	324	680	2449	1508
w.r.t. $\sigma = 5$ mm and $\alpha$	132	316	579	759	633	1410	3449	2960

## Discussion

In this work we presented a study designed to quantify the uncertainties related to the variability in scanning conditions when measuring brain tumor sizes on MRI. Given the rare occurrence of the pathology, and the cost of such study, it is not possible to acquire a large database of MRI images on low-grade glioma patients scanned with different axial plane orientations and slice thicknesses. We therefore opted for a simulation framework of these two scanning conditions.

A comprehensive set of experiments, exploiting a large database of manually segmented low-grade gliomas, was performed to evaluate the uncertainties of two tumor size index measures: the bi-dimensional diameter product index, used for response assessment in neuro-oncology [8, 10, 14], and the equivalent diameter index, used in radiological longitudinal monitoring of low-grade glioma growth [2, 9].

As an outcome of our study, we observed that the upper bounds of measurement variability under varying scanning conditions highly depend on the size of the tumor. We summarized these upper bounds expressed in percent (Table 1) and mm (Table 2), for the two most common large slice thickness values used in clinical setting (3 and 5mm), dividing the tumors into four volume categories.

These results confirm that the bi-dimensional diameter product  $BP$  is very sensitive to scanning conditions. Hence, a minor response (defined by a 25 % decrease of  $BP$ ) might be observed as a pure effect of variability in scanning conditions, leading to erroneous classification of a patient as a responder while the tumor volume is in fact unchanged.

On the other hand, the volume-based index  $D_{eq}$  shows greater stability over the different scanning conditions for all tumor size categories. In particular, it is interesting to note that the maximal variability of the  $D_{eq}$  size index is close to 1mm for tumors with a diameter greater than 20mm (typical size in preoperative screening). This 1mm

variability sets the limits of the accuracy one can reach when estimating quantitatively the tumor size evolution on two longitudinal MRI examinations performed with different orientations of the axial plane. For tumors with diameter smaller than 20mm (typical size of postoperative residues), the maximal variability of the  $D_{eq}$  size index is comprised between 2 and 3mm, which precludes any reliable estimation of growth rates. These results, which await confirmation on a series of real patients being scanned with FLAIR MRI, highlight the importance of defining standard guidelines for the choice of the MRI axial plane orientation and positioning of a reference slice that could be easily applied across any institution. Automated methods for reproducible axial slice positioning could be easily implemented in the near future [15–17]. As a manual alternative, the axial plane joining the knee to the splenium of the corpus callosum (on the mid-sagittal view of the corpus callosum) could define a slice of reference to acquire, leading to a simple guideline to follow (see Fig. 1).

Finally, this paper contributes to the enforcement of volume segmentation methods rather than the currently recommended two largest diameters method when assessing glioma size evolution on MRI [8, 18]. Initial recommendations to use the two largest diameters method go back to the time when MRI images were printed and not accessible in the DICOM format. Several studies since then have demonstrated the unreliability of this method, due to high inter-observer [10] and intra-observer [19] variability. Volume segmentation methods can now be easily implemented on any workstation with a DICOM viewer, and such measure should be part of the standard of care, despite the fact that it is more time-consuming. Hopefully, advances in semi-automated brain tumor segmentation tools should help overcome this limitation.

In conclusion, patient follow up using MRI scans with large slice thickness (3 mm and above) requires precise control and replication of the patient's head position to quantify tumor growth from size index measures. The two largest diameters method is not appropriate for large MRI slice thickness, even when patient's head position is controlled. The studied volume segmentation method provides reliable measures for growth quantification of tumors above a certain size. For small tumors, exact replication of scanning conditions is mandatory.

**Conflict of interest** We declare that we have no conflict of interest.

## References

- Caseiras G, Ciccarella O, Altmann DR, Benton CE, Tozer DJ, Tofts Paul S, Yousry TA, Rees J, Waldman AD, Jger HR (2009) Low-grade gliomas: Six-month tumor growth predicts patient outcome better than admission tumor volume, relative cerebral blood volume, and apparent diffusion coefficient. *Radiology* 253(2):505–512
- Mandonnet E, Delattre JY, Tanguy Marie-Laureand Swanson, KR, Carpentier AF, Duffau H, Cornu P, Van Effenterre R, Alvord EC, Capelle L (2003) Continuous growth of mean tumor diameter in a subset of grade II gliomas. *Ann Neurol* 53(4):524–528
- Pallud J, Mandonnet E, Duffau H, Kujas M, Guillemin R, Galanaud D, Taillandier L, Capelle L (2006) Prognostic value of initial magnetic resonance imaging growth rates for world health organization grade II gliomas. *Ann Neurol* 60(3):380–383
- Mandonnet E, Pallud J, Fontaine D, Taillandier L, Bauchet L, Peruzzi P, Guyotat J, Bernier V, Baron MH, Duffau H, Capelle L (2010) Inter- and intrapatient comparison of WHO grade II glioma kinetics before and after surgical resection. *Neurosurg Rev* 33:91–96
- Peyre M, Cartalat-Carel S, Meyronet D, Ricard D, Jouvret A, Pallud J, Mokhtari K, Guyotat J, Jouanneau E, Sunyach MP, Frappaz, D, Honnorat J, Ducray F (2010) Prolonged response without prolonged chemotherapy: a lesson from PCV chemotherapy in low-grade gliomas. *Neuro-Oncology* 12(10):1078–1082
- Ricard D, Kaloshi G, Amiel-Benouaich A, Lejeune J, Marie Y, Mandonnet E, Kujas M, Mokhtari K, Taillibert S, Laigle-Donadey F, Carpentier AF, Omuro A, Capelle L, Duffau H, Cornu P, Guillemin R, Sanson M, Hoang-Xuan K, Delattre JY (2007) Dynamic history of low-grade gliomas before and after temozolomide treatment. *Ann Neurol* 61(5):484–490
- Pallud J, Llitjos JF, Dhermain F, Varlet P, Dezamis E, Devaux, B, Souillard-Scmama R, Sanai N, Koziak M, Page P, Schlienger M, Daumas-Duport C, Meder JF, Oppenheim C, Roux FX (2012) Dynamic imaging response following radiation therapy predicts long-term outcomes for diffuse low-grade gliomas. *Neuro-Oncology* 14(4):496–505
- van den Bent M, Wefel J, Schiff D, Taphoorn M, Jaeckle K, Junck L, Armstrong T, Choucair A, Waldman A, Gorlia T, Chamberlain M, Baumert B, Vogelbaum M, Macdonald D, Reardon D, Wen P, Chang S, Jacobs A (2011) Response assessment in neuro-oncology (a report of the RANO group): assessment of outcome in trials of diffuse low-grade gliomas. *The Lancet Oncol* 12(6):583–593
- Pallud J, Taillandier L, Capelle L, Fontaine D., Peyre M, Ducray F, Duffau H, Mandonnet E (2012) Quantitative morphological MRI follow-up of low-grade glioma: a plea for systematic measurement of growth rates. *Neurosurgery*
- Sorensen AG, Patel S, Harmath C, Bridges S, Synnott J, Sievers A, Yoon YH, Lee EJ, Yang MC, Lewis RF, Harris GJ, Lev M, Schaefer PW, Buchbinder BR, Barest G, Yamada K, Ponzio J, Kwon HY, Gemmete J, Farkas J, Tievsky AL, Ziegler RB, Salhus MR, Weisskoff R (2001) Comparison of diameter and perimeter methods for tumor volume calculation. *J Clin Oncol* 19(2):551–557
- Mandonnet E, Pallud J, Clatz O, Taillandier L, Konukoglu, E, Duffau H, Capelle L (2008) Computational modeling of the WHO grade II glioma dynamics: Principles and applications to management paradigm. *Neurosurg Rev* 31:263–269
- Mandonnet E, Jbabdi S, Taillandier L, Galanaud D, Benali H, Capelle L, Duffau H (2007) Preoperative estimation of residual volume for WHO grade II glioma resected with intraoperative functional mapping. *Neuro-Oncology* 9(1):63–69
- Alfano B, Comerci M, Larobina M, Prinster A, Hornak JP, Selvan SE, Amato U, Quarantelli M, Tedeschi G, Brunetti A, Salvatore M (2011) An MRI digital brain phantom for validation of segmentation methods. *Med Image Anal* 15(3):329–339
- Macdonald DR, Cascino TL, Schold SC, Cairncross JG (1990) Response criteria for phase II studies of supratentorial malignant glioma. *J Clin Oncol* 8(7):1277–80

15. Chen T, Zhan Y, Zhang S, Dewan M (2011) Automatic alignment of brain MR scout scans using data-adaptive multi-structural model. In: Medical image computing and computer-assisted intervention (MICCAI) 2011. LNCS. Springer, New York, vol 6892, pp 574–581
16. Gedat E, Braun J, Sack I, Bernarding J (2004) Prospective registration of human head magnetic resonance images for reproducible slice positioning using localizer images. *J Magn Resonan Imaging* 20(4):581–587
17. Van der Kouwe AJ, Benner T, Fischl B, Schmitt F, Salat DH, Harder M, Sorensen AG, Dale AM (2005) On-line automatic slice positioning for brain MR imaging. *NeuroImage* 27(1): 222–230
18. Wen PY, Macdonald DR, Reardon DA, Cloughesy TF, Sorensen AG, Galanis E, DeGroot J, Wick W, Gilbert MR, Lassman AB, Tsien C, Mikkelsen T, Wong ET, Chamberlain MC, Stupp R, Lamborn KR, Vogelbaum MA, van den Bent MJ, Chang SM (2010) Updated response assessment criteria for high-grade gliomas: response assessment in neuro-oncology working group. *J Clin Oncol* 28(11):1963–1972
19. Provenzale JM, Ison C, DeLong D (2009) Bidimensional measurements in brain tumors: Assessment of interobserver variability. *Am J Roentgenol* 193(6):W515–W522